NACA

RESEARCH MEMORANDUM

HEAT TRANSFER AND PRESSURE DISTRIBUTION AT A MACH

NUMBER OF 6.8 ON BODIES WITH CONICAL FLARES

AND EXTENSIVE FLOW SEPARATION

By John V. Becker and Peter F. Korycinski

Langley Aeronautical Laboratory
Langley Field, Va.

This material contains information affecting the National Defense of the United States within the meaning
of the espionage laws, Title 18, U.S.C., Secs. 793 and 794, the transmission or revelation of which in any
manner to an unauthorized person is prohibited by law.

NATIONAL ADVISORY COMMITTEE
FOR AERONAUTICS
WASHINGTON
July 20, 1956

H

NACA RM L56F22

NATIONAL ADVISORY COMMITTEE FOR AERONAUTICS

RESEARCH MEMORANDUM

HEAT TRANSFER AND PRESSURE DISTRIBUTION AT A MACH

NUMBER OF 6.8 ON BODIES WITH CONICAL FLARES

AND EXTENSIVE FLOW SEPARATION

By John V. Becker and Peter F. Korycinski

SUMMARY

An investigation of heat transfer and pressure distribution on flared bodies under laminar, transitional, and turbulent boundary-layer conditions was conducted in the Langley 11-inch hypersonic tunnel at a Mach number of 6.8. The results indicated extensive zones of separated flow ahead of the flares when the boundary layer was laminar at separation. The rate of heat transfer in these zones was found to be considerably less than in attached laminar flow except in regions where transition occurred on the separated boundary.

In the turbulent cases the separated zone was so localized as to be undiscernible in schlieren photographs. Downstream of flow reattachment on the flare, the Stanton number based on local conditions was found to be several times greater for large flare angles than the values existing in attached flow on the body ahead of the flare.

The results are analyzed to determine the adequacy of available theoretical methods for predicting heat transfer in cases where the transition point and the limits of the separated zone are known.

INTRODUCTION

The flared or flapped surfaces contemplated for controlling the drag or stability of hypersonic aircraft present a serious heating problem, probably second in importance only to that of the body nose and wing leading edge. Basically, the problem is more complex than that of the leading edge because of the occurrence of shock—boundary-layer interaction with separation.

A considerable background of theory and experiment has been built up for the lower supersonic speed range which establishes the general

CONFIDENTIAL

character of this interaction process. (For example, see refs. 1 to 10.) However, the heat transfer in this critical area is largely unknown. In some cases it has been surmised that the heat-transfer rate may be aggravated by separation while in others it has been postulated that the separated zone might have an insulating effect. Tests which might be construed to support the former viewpoint are described in reference 11, in which the effect of a spike protruding ahead of a spherical nose was to increase the heat transfer above the laminar level found in unseparated flow without the spike. These results are not completely conclusive, however, because of the possibility that the spike may have triggered transition. Furthermore, it is probable that the results obtained on the bluff body at the end of the separated zone produced by the spike are not similar to what would be found on a cylindrical or conical surface.

Aside from the foregoing questions pertaining to the separated zone, the heat transfer in attached flow on a flare or flap cannot be calculated theoretically at present because of inadequacies in current theories for predicting boundary-layer-profile changes through the phenomena found at the body-flare juncture. Thus, the need for research in this area is obvious. The only previous experimental work known to the authors consists of flight temperature measurements at two stations on a wing flap under conditions of fully turbulent (and probably unseparated) flow (ref. 12). For the small flap angle of these tests ($10°$) the Stanton number based on local conditions on the flap appeared to be approximately the same as on the wing just ahead of the flap.

The material presented in the present paper is drawn from a current program in the Langley 11-inch hypersonic tunnel at $M = 6.8$ which utilizes a typical ogive cylinder with various conical flared skirts. The purpose of this investigation is to establish the character of the interaction and heat-transfer phenomena for conditions of laminar, transitional, and turbulent boundary layers ahead of the flare. This paper presents the results of initial experiments with models having $10°$ and $30°$ flares.

The tests were conducted by various members of the 11-inch hypersonic tunnel staff including Messrs. C. H. McLellan, Mitchel H. Bertram, Davis H. Crawford, and David E. Fetterman, Jr. Mr. Crawford also assisted in the analysis of the results by applying the method of Stine and Wanlass to obtain the theoretical laminar heat transfer for the ogival nose.

SYMBOLS

c chord of flare

C_D pressure-drag-coefficient increment due to flare, $\dfrac{\text{Pressure-drag increment}}{\left(\pi D^2/8\right)\rho_o V_o{}^2}$

C_p pressure coefficient, $\dfrac{p_l - p_o}{\rho_o V_o^2/2}$

c_p specific heat at constant pressure

D diameter of cylindrical part of body

L overall length of model

M Mach number

p pressure

p'_3 theoretical pressure at reattachment point (two dimensional)

q heat transferred per unit area

R radius

R_D Reynolds number based on free-stream conditions and body diameter, $\rho_o V_o D/\mu_o$

R_L Reynolds number based on free-stream conditions and model length, $\rho_o V_o L/\mu_o$

R_{x_t} Reynolds number based on free-stream conditions and distance to transition point x_t, $\rho_o V_o x_t/\mu_o$

St Stanton number based on free-stream conditions, $\dfrac{q}{c_{p_o}\rho_o V_o\left(T_r - T_w\right)}$

St_l Stanton number based on local conditions, $\dfrac{q}{c_{p_l}\rho_l V_l\left(T_{r_l} - T_w\right)}$

T temperature

T_r recovery temperature

T_w skin temperature

t time

4

CONFIDENTIALCONFIDENTIAL

NACA RM L56F22

V   velocity

x   axial distance

s   distance along surface of flare

δ   flare deflection angle

μ   viscosity

ρ   density

Subscripts:

o   free-stream condition (or zero time on fig. 2 only)

l local condition

1   station immediately ahead of separation point on cylinder
         (fig. 5)

2   station in separated-flow region where "plateau" pressure
         occurs (fig. 5)

3   station on flare immediately downstream of assumed flow reat-
         tachment point (fig. 5)

APPARATUS AND METHODS

The experiments were made in the Langley 11-inch hypersonic tunnel which is described in reference 13. The storage heater has been replaced by an electric heater and the tunnel now has invar nozzle blocks (see ref. 14) which have largely eliminated the test-section Mach number variation with time due to warpage of the nozzle throat. All experiments were made at 0° angle of attack and a tunnel stagnation temperature of about 1,100° R. Tunnel stagnation pressure was varied from 3.2 to 42.9 atmospheres. At the lowest pressure, 3.2 atmospheres, the Mach number was 6.52 and it gradually increased to 6.88 at the higher stagnation pressures.

Ogive-cylinder models with 10° and 30° flared tails were used in these experiments. The nose was a Von Kármán minimum-drag shape of fineness ratio 5 with a 10° half-angle cone at the tip. The midbody was a cylinder 5 diameters long. The flared skirts were about 2 diameters long. Overall length of the models was about 18 inches and the diameter of the cylinder was 1.5 inches. Figure 1 shows the model coordinates and the locations of the pressure orifices.

CONFIDENTIALCONFIDENTIAL

Separate models were used for pressure and temperature measurements. Pressure models were conventional, and pressure measuring and recording equipment similar to that of reference 15 was used. The initial temperature model (10° flare) was spun from Inconel X. Its skin thickness varied from about 0.030 to 0.050 inch. In computing heat transfer the actual local skin thicknesses were used. The temperature model with 30° flare was machined from mild steel to a uniform skin thickness of 0.030 ± 0.001 inch.

The temperature models were equipped with chromel-alumel thermocouples (no. 36 wire) affixed with silver solder to the undersurface of the skin. Temperatures were recorded on self-balancing recording potentiometers. A maximum of four thermocouples were connected to each recorder, and the thermocouple readings were recorded once every 4 seconds. The locations of the thermocouples are shown in figure 1.

Schlieren observations were made of the flow about both pressure and temperature models. Photographs of the flow about the model with 10° flare were made with an exposure of about 4 microseconds; the exposure used for the models with 30° flare was about 1/150 second.

The method of determining heat-transfer rates was as follows. By preliminary stabilization of the electric tunnel-air heater (passing air through the heater but not through the nozzle), it was possible to approximate a step-function type of air-temperature variation·from an initial temperature without flow of about 535° R for the model and tunnel air to the tunnel stagnation temperature of about $1,100^\circ$ R. In figure 2 is shown a typical skin-temperature history at a given station. The slope of the curve at zero time is determined by extrapolation, a small correction to the first few data points being necessary to account for the fact that the air-temperature curve is not a true step function.

This method has two important advantages: (1) Heat transfer is determined for the isothermal skin-temperature case, which is the most basic and most easily specified case and the only case for which many current theories apply. (2) No skin-conduction corrections are necessary, a fact which greatly facilitates data reduction.

The accuracy of the method depends to a large extent on the frequency with which reliable thermocouple readings are recorded near the beginning of the run. With the equipment used, one measurement every 4 seconds appeared to give an overall accuracy adequate for these initial experiments. An assessment of the accuracy can be obtained by comparing measurements made on the ogival nose in several test runs (fig. 5). Two runs made at nearly the same Reynolds number (fig. 5(c)) can also be compared. The method can obviously be made more accurate by taking measurements at shorter time intervals.

DISCUSSION

Flow Characteristics

At the lower test Reynolds numbers extensive laminar separation occurred ahead of the flare, as illustrated in figure 3 for the 30° flare at $R_L = 1.8 \times 10^6$. For this case the entire cylindrical portion of the body and nearly all of the flare were immersed in the separated flow. Transition to turbulent flow appeared to start on the outer boundary of the separated region at a considerable distance downstream of the separation point. At the highest test Reynolds number, $R_L = 8.3 = 10^6$ $\left(\text{or } R_D = 0.69 \times 10^6\right)$, transition started ahead of the separation point (at $x/D = 6.5$), and was completed ahead of the body-flare juncture. The flow for this turbulent condition is pictured on the right side of figure 3. No separation is visible in this picture, although a small bubble of separation presumably exists at the flare juncture since the pressure rise, $\Delta p/p_1 \approx 20$, is far greater than that estimated for turbulent separation ($\Delta p/p_1 \approx 4$, refs. 7 to 10). The critical dependence of these separation characteristics on whether the boundary layer was laminar or turbulent at separation is consistent with previous findings at lower Mach numbers (e.g., ref. 9).

The manner in which the observed locations of separation and transition varied with test Reynolds number is also qualitatively consistent with previous work. Also, following previous work, the flow regime will be referred to as "laminar" in the range of Reynolds numbers for which the boundary layer over the entire separated-flow zone is laminar, "transitional" for Reynolds numbers at which transition occurs on the separated-flow boundary, and "turbulent" for Reynolds numbers at which the transition point is ahead of the separation point. Figure 4(a), for the 10° flare, shows that the laminar regime prevailed at the lowest Reynolds numbers. As the Reynolds number was increased the separation point at first moved upstream; this is apparently a characteristic of purely laminar separations (ref. 9). The dashed line in figure 4(a) shows this trend as predicted by reference 9 for lower supersonic speeds. As transition moved forward onto the separated zone this trend reversed, and finally, with transition ahead of separation, the very small separation distances characteristic of turbulent flow prevailed. The data points on the "transition point" curve of figure 4(a) denote the location of the start of transition and were obtained from both heat-transfer data and schlieren photographs.

Similar results were obtained for the $30°$ flare (fig. 4(b)) with the principal exception that for R_D greater than 0.14×10^6 the boundary layer remained laminar only to about the 8.3D body station in the presence of the large destabilizing separated zone. At lower Reynolds numbers the flow regime may be laminar, as indicated by the initial forward movement of the separation point. However, because heat-transfer data were not obtained in this range and because the air-stream density was too low for reliable use of the schlieren photographs, the existence of laminar flow was not confirmed. At higher Reynolds numbers the location of the start of transition on the boundary (determined from schlieren pictures) remained approximately fixed with increasing test Reynolds number until the separation point had moved downstream of transition. Similar results for a two-dimensional transitional case are described in reference 9 for $M = 2$ to 4.

It should be noted that the technique used to locate transition on the outer boundary of the separated flow (by inspection of a considerable number of schlieren photographs) became increasingly unreliable as the Reynolds number (density) was reduced. It is probable, however, that the mean locations shown in figure 4(b) are correct to within 1 diameter. Where transition was well ahead of separation, the start of transition could be detected accurately from the temperature measurements because in this case there was no possibility of confusing transition and separation effects.

It was noticed that the extent of the separated region fluctuated rapidly when the transition location on the separated boundary was in the vicinity of the separation point. These fluctuations of course resulted in corresponding large and rapid variations in the pressures on the flared surface. This apparent coupling between the fluctuations of the transition point and the extent of the separated region provides an obvious reason for the lower transition Reynolds numbers existing in the presence of extensive separation. For the model with $30°$ flare, for example, the transition Reynolds number R_{x_t} varied from about 1.2×10^6 in the presence of the longest separated zone to about 4.7×10^6 when the transition and separation points coincided. (See fig. 4(b).) In the absence of separation, transition Reynolds numbers varying between 4.5×10^6 and 5.1×10^6 were observed, values in the same range as previously found in this wind tunnel on a cylindrical body (ref. 16).

Heat Transfer

Method of presentation.- The Stanton number based on free-stream conditions is used in presenting the results (fig. 5) because it

indicates directly the large variations in local heat-transfer rate occurring along the length of the body. For the regions of laminar flow over the forward part of the body, data obtained at different test pressures can be correlated through use of the parameter $St/\overline{R_D}$ which is used in figure 5. In regions of turbulent flow, of course, a different value of this parameter exists for each test Reynolds number. In reducing the experimental data to values of $St/\overline{R_D}$, a laminar recovery factor of 0.84 based on free-stream conditions was used for all points, except those on the flare itself for cases in which it was known that the flare boundary layer was fully turbulent. In these cases a recovery factor of 0.90 was used, a value appropriate for turbulent flow under the existing tunnel conditions.

Because of the controlling effect of local pressure on the local heat-transfer rate, a plot of the pressure distribution along the body is included below each of the heat-transfer diagrams in order to aid in the interpretation of the results. The theoretical pressure distribution on the ogive and cylinder was calculated by the method of characteristics and was used with the method of Stine and Wanlass (ref. 14) to obtain the theoretical values of the laminar heat-transfer coefficients. Pressures on the flare were estimated by wedge and cone theory. When little or no apparent separation was evident, the flow approximated inviscid flow, and the two-dimensional pressure at the flare-body juncture designated as "p_3 - wedge" and the three-dimensional "cone" pressure (see fig. 5(a)) were calculated by starting with the theoretical pressure on the cylinder $\left(C_{p_{cyl}}\right.$ was taken as $-0.005\left.\right)$. When separation was present, the theoretical pressure at reattachment p'_2 was calculated by starting with the experimental pressure in the separated region, p_2, and the deflection angle was taken as the flare angle minus the measured separation wedge. The measured separation angles used were 3° for the model with 10° flare and 7° for the model with 30° flare. In the heat-transfer calculation the wedge pressures were used and were assumed to apply over the entire flare chord.

In using the method of Van Driest (ref. 17) to calculate the theoretical laminar flat-plate heat-transfer coefficients for the cylinder and the flare, it is necessary to account for the difference between the reference static temperature of 392° R used by Van Driest and the static temperature in the tunnel, which in the case of the 11-inch hypersonic tunnel is about 110° R. For an insulated flat plate the correction factor is 1.22, and this factor was applied to the theoretical values with the assumption that it remains constant over the range of wall-temperature to static-temperature ratios covered in this investigation. For the turbulent case the methods of reference 18 were applied.

Laminar case, 10° flare.- Figure 5(a) presents the results obtained at a low Reynolds number for which the flow was laminar over the entire body. On the cylindrical part of the body the compressible laminar theory (ref. 17) was used with an assumed starting point at $x/D = 1.75$, which resulted in agreement with the nose calculations at the nose-cylinder juncture. Reasonable agreement between both the heat-transfer and pressure data and the theoretical estimates is shown up to the separation point.

In the separated region it is shown in figure 5(a) that the heat-transfer rate decreases to roughly 50 percent of the level that would exist in unseparated flow (solid line). This decrease occurs in spite of the increase in pressure caused by the presence of separation; the dashed line labeled "laminar - p_2" is the approximate heat-transfer level that would be expected for unseparated flow on the cylinder at the pressure p_2. Whether this decrease is due to a reduction in recovery factor or a reduction in local heat-transfer coefficient (or more probably a reduction in both factors) is not known, since local recovery factor was not measured. It is clear, however, that this purely laminar separation results in a marked decrease in heat-transfer rate.

No satisfactory theoretical method was found for estimating the heat-transfer rate on the flare. The flow in the vicinity of the flare-cylinder juncture presents an extremely complex problem because the velocity profile is subject to large distortions from the occurrence of shock interaction, separation, mixing, and reattachment. For large ratios of flare length to body length and for large flare deflections, it might be expected that the body boundary-layer effects would be secondary. Thus it was assumed that the flare boundary layer started at the point of reattachment, as a basis for rough estimates of the flare heat-transfer levels for figure 5. In the particular separated case considered in figure 5(a) the pressures on the flare were initially much below the theoretical values for inviscid flow because of the manner in which the boundary layer bridged the juncture. This accounts for the fact that the heat-transfer level is far less than estimated for the theoretical (inviscid) pressure at reattachment. Near the trailing edge better agreement is evident for both pressure and heat transfer.

Turbulent case, 10° flare.- Results for a high test Reynolds number in which transition was essentially completed ahead of the juncture are shown in figure 5(b). In calculating the theoretical turbulent heat transfer on the cylinder for this case the usual assumption was made that the momentum in the boundary layer was constant across transition. On the flare, the turbulent boundary layer was assumed to start at the juncture, and flat-plate values for the theoretical flow conditions just aft of the juncture were obtained from reference 18.

Apparently, under the conditions of figure 5(b) transition required about 3 body diameters of distance before "fully developed" turbulent flow was established. Because of the action of the relatively thick boundary layer the pressure started to rise just ahead of the flare and at the midchord was closer to the wedge pressure than the cone pressure. As in the laminar case, the heat-transfer results reflect the characteristics of the experimental pressure diagram. There was no evidence of a "hot spot" in the flare-body juncture.

Turbulent case, 30° flare.- These results (fig. 5(c)) are similar to those for the turbulent case for the 10° flare (fig. 5(b)) with the exception that both the pressures and the heat-transfer rates achieve peak values on the flare somewhat in excess of the estimates obtained theoretically by using the wedge pressures. It is thought that the boundary layer, including the probable presence of a small bubble of separation, bridges the juncture in such a way as to cause a continuous pressure rise which makes possible a higher pressure peak than that of the single strong shock visualized in the inviscid theory.

Transitional case, 30° flare.- Figure 5(d) presents the results obtained at a low Reynolds number in which extensive separation was present. As mentioned previously, this case involved laminar separation followed by transition starting about 1.7 diameters ahead of the flare. It will first be noted that the pressures in the separated flow on the flare are extremely low. The pressure rises on approaching the reattachment point, and it was assumed that the theoretical wedge pressure level was attained although the lack of pressure orifices in this area makes it impossible to confirm this assumption. Estimates of heat-transfer rate agree surprisingly well with the test results in view of the arbitrary assumptions involved.

Perhaps the most significant result for this transitional case is the rapid increase in heat transfer which starts to occur within the region of separated flow near the location of transition on the outer boundary. In the previously illustrated case of pure laminar separation (fig. 5(a)), there was no such rise above the estimated heat-transfer level for attached laminar flow. There is thus a marked difference in the heat-transfer characteristics of separated-flow zones, depending on whether transition occurs. This result suggests the speculation that the adverse effect of separation on heat transfer to a spherical nose which was observed by Stalder and Neilsen (ref. 11) may have been due to the occurrence of transition.

Local heat-transfer coefficients on flare.- In areas on the flare where the flow is separated or transitional or both, it is evident from figures 5(a) and (d) that the pressure as well as the heat transfer is subject to large and quantitatively unpredictable variations. In the simpler turbulent cases (e.g., those of figs. 5(b) and (c)) or in

separated cases where only the part of the flare downstream of reattachment is considered and where the flow is known to be either laminar or turbulent, there is some hope that a method of prediction of local heat transfer can be developed. As pointed out previously, however, even in these simpler cases theoretical determination of the distortions of the velocity profile in the flow at the juncture presents a complex unsolved problem. In these simpler cases the local pressure and other conditions outside the boundary layer are predictable, to a first order of approximation at least, when the separation and reattachment points are known, but the boundary-layer parameters governing the local heat-transfer coefficient are not calculable.

Previous investigators have used the following widely different arbitrary assumptions in attempts to estimate approximately the local heat-transfer coefficient on flared or flapped surfaces:

(1) St_l assumed constant across the juncture

(2) Momentum of the boundary layer assumed constant across the juncture; no change in velocity profile shape

(3) Momentum thickness of the boundary layer assumed constant across the juncture; no change in velocity profile shape

Assumption (1) is shown by the present results to be completely invalid except for very small flare angles. Figure 6 indicates that the peak Stanton number based on local (wedge) conditions on the flare is 3.5 times the undeflected value for the 30° flare and 1.2 times the undeflected value for the 10° flare. The application of assumptions (2) and (3) for the 30° flare produced the two dashed curves shown in figure 6. The assumption (2) of constant momentum across the juncture naturally results in a thinner boundary layer and higher heat transfer than the assumption (3) of constant momentum thickness. The fact that the experimental points fell above case (2) suggested the approximation used in this paper (fig. 5) in which the boundary layer from the forebody is neglected and it is assumed that the flare boundary layer starts at the juncture. This latter method of course results in infinite heat-transfer coefficient at the juncture, but if the first 10 percent of the flare chord is neglected, it produces somewhat better agreement than the other arbitrary methods. Obviously, this method should provide increasingly accurate predictions as the ratio of flare chord to body length increases, and as the flare angle increases. For small flare angles, however, the assumption that the body boundary layer can be neglected becomes increasingly untenable, obviously being completely invalid at $\delta_f = 0$. It is quite evident that further experimental and analytical work on this problem is necessary.

Flare Drag

The variation of extent of separation with Reynolds number obviously affects the amount of pressure drag produced by the flare. The large magnitude of this effect is shown in figure 7, where the data for both configurations are based on the same axial flare lengths ($\Delta x/D = 2$). The abrupt increase in drag for the 30° flare at a Reynolds number of about 0.15×10^6 apparently occurs when the reattachment point starts to move forward from the rear edge of the flare. In the case of the 10° flare, within the accuracy of the data, the drag appeared to increase continuously after the separation point had started to move rearward (cf. figs. 4 and 7).

The use of simple inviscid theory to predict flare drag is obviously unjustifiable in the presence of extensive separation. It will be noticed, however, that at the higher Reynolds numbers, where no significant separation occurred, the experimental data fell between the theoretical levels calculated by using inviscid wedge and cone pressure coefficients for the flares. The experimental data were in closer agreement with the wedge pressure levels.

Relation Between Flare Drag and Flare Heating

The results previously discussed indicated major changes in both flare drag and flare heat transfer with the extent and character of separated flow. If the objective of the flare is to produce drag, it is of interest to inquire what condition of the separated zone will result in maximum values of the ratio of flare drag to average flare heat transfer. With the mean Stanton number based on stream conditions $\overline{St}$, it is desirable that $C_D/\overline{St}$ be a maximum. For unseparated flow this parameter would theoretically increase with flare angle, and for a given flare angle it would, of course, be theoretically much larger with laminar than with turbulent heat transfer. Since extensive separation and low drag exist in the actual laminar case, however, it remains for experiment to determine whether this case has any real advantage.

In figure 8, the calculated values of $C_D/\overline{St}$ for both a laminar (low Reynolds number) and a turbulent (high Reynolds number) condition are presented. Two-dimensional flow was assumed in calculating local conditions. The mean Stanton numbers correspond to local Reynolds numbers at the midchord line of the flare ($x/D = 11$) with the boundary layer starting from the body-flare juncture. As for the experimental results, the mean Stanton number was obtained from integration of the local Stanton numbers on the flare, assuming a flare axial length of $\Delta x/D = 2$; the corresponding values of pressure drag were obtained from the faired

curves of figure 7. It is seen that for the 10° flare the experimental values of $C_D/\overline{St}$ were in agreement with the theoretical estimates both in fully laminar flow at the lower Reynolds numbers and in the turbulent flow at the higher test Reynolds numbers. In this case the zone of separation covered only the forward 20 percent of the flare chord at the lowest Reynolds number (fig. 5(a)).

For the 30° flare with laminar separation, nearly the entire chord was submerged in separated flow at the lower Reynolds numbers, and the high ratio of drag to heat transfer calculated for laminar flow was not realized. In fact, by a considerable margin the highest ratio of drag to heating is achieved with turbulent flow. The very low values of $C_D/\overline{St}$ obtained for the 30° flare at the lowest Reynolds numbers are a consequence of the low drag resulting from extensive laminar separation and the high heat transfer existing in the transitional flow over the flare. If the flow had remained laminar on the separated boundary a more favorable value of $C_D/\overline{St}$ would have been obtained at the lower Reynolds numbers because of reduced heat transfer, while the drag presumably would not have been much affected in this case. Calculations for this fully laminar separated-flow case indicate, however, that the value of $C_D/\overline{St}$ would still be only about one-half the value for the turbulent or high Reynolds number. It is thus clear that for this high-flare-angle configuration it is advantageous to prevent laminar separation, even if this is accomplished by tripping the boundary layer to produce turbulent flow.

The basic reason for the superiority of the turbulent case lies in the fact that only a small fraction of the drag energy of a 30° flare appears as flare heating. It is therefore beneficial to achieve the high attached-flow drag even if this involves a change from laminar to turbulent heat-transfer level on the flare.

It should be made clear in conclusion that the turbulent-flow case will produce more favorable values of $C_D/\overline{St}$ only for configurations where the drag suffers a major decrease due to laminar separation, that is, only where a major part of the flare area is immersed in the separated zone in the laminar case.

CONCLUDING REMARKS

The flow-separation phenomena observed at $M = 6.8$ on bodies of revolution with conical flared skirts were similar in character to previously observed separated flows on flat plates with flaps or wedges investigated at lower Mach numbers. In particular, large zones of

separation existed ahead of the flare in the case of laminar flow, while in the turbulent case the separated region was too short to be visible in schlieren pictures. The flare pressure distributions and drag were accordingly much closer to the theoretical inviscid-flow values in the turbulent case.

The presence of separated flow appeared to cause a reduction in transition Reynolds number in all cases. For the most extensive separated zone (flare angle of 30°) the laminar boundary layer persisted along the outer boundary of the separated flow to a Reynolds number of about 1.2×10^6 at which transition appeared to start. As the separated zone diminished in length with increasing Reynolds number, the transition Reynolds numbers increased to a maximum of about 5×10^6 in the absence of separation. In the transitional cases the flow became increasingly unsteady as the transition and separation points drew closer together with increasing Reynolds number.

Heat-transfer measurements in a case in which the flow was laminar over the entire model indicated that the rate of heat transfer in the separated zone was roughly half that for attached flow. However, when transition occurred on the outer boundary of the separated zone the heat transfer to the surface increased rapidly with distance downstream from the transition point. There was no evidence of a hot spot in the juncture for the case of turbulent separation. On the flare the measured Stanton numbers based on local conditions were much larger than for the undeflected case - for example, about three times as great for a 30° flare in turbulent flow.

In absence of separation the heat-transfer rates over the body ahead of the flare could be predicted theoretically with satisfactory accuracy when the transition location was known, except in the transition region. No adequate theoretical method is available to predict the local heat-transfer coefficients on the flare. A crude approximation suggested by the experimental results, however, can be used for large flare angles to establish the order of the local heat-transfer coefficients. In this approximation the assumption that the flare boundary layer started at the point of flow reattachment produced local Stanton numbers of the right order over about 90 percent of the flare chord downstream of the reattachment point. Obviously, this approximation is not valid for small flare deflections and further analytical work on this problem is needed.

For flare angles of the order of 30° it was found that for a given drag increment less heat was transferred to the flare in turbulent-flow cases than in the cases involving laminar separation. This result was a consequence of the much higher drag coefficient achieved in the (attached-flow) turbulent cases, which more than offsets the higher heat-transfer coefficients in turbulent flow. It is to be expected that this result holds only for the laminar cases in which a major part of the flare chord is immersed in the separated zone.

Langley Aeronautical Laboratory,
      National Advisory Committee for Aeronautics,
            Langley Field, Va., June 4, 1956.

REFERENCES

1. Ackeret, J., Feldmann, F., and Rott, N.: Investigations of Compression Shocks and Boundary Layers in Gases Moving at High Speed. NACA TM 1113, 1947.

2. Lees, Lester: Interaction Between the Laminar Boundary Layer Over a Plane Surface and an Incident Oblique Shock Wave. Rep. No. 143, Princeton Univ., Aero. Eng. Lab., Jan. 24, 1949.

3. Lee, J. D.: The Influence of High Adverse Pressure Gradients on Boundary Layers in Supersonic Flow. UTIA Rep. No. 21, Univ. of Toronto, Inst. Aerophysics, Oct. 1952.

4. Gadd, G. E.: A Simple Theory for the Interactions Between Shock Waves and Entirely Laminar Boundary Layers. Rep. No. F.M. 2003, British N.P.L. (Rep. No. 16,416, A.R.C.), Dec. 15, 1953.

5. Ritter, Alfred, and Kuo, Yung-Huai: Reflection of a Weak Shock Wave From a Boundary Layer Along a Flat Plate. I - Interaction of Weak Shock Waves With Laminar and Turbulent Boundary Layers Analyzed by Momentum - Integral Method. NACA TN 2868, 1953.

6. Gadd, G. E., and Holder, D. W.: The Interaction of an Oblique Shock Wave With the Boundary Layer on a Flat Plate. Part I. Results for M = 2. Rep. No. F.M. 1714, British N.P.L. (Rep. No. 14,848, A.R.C.), Apr. 24, 1952.

7. Bogdonoff, S. M., Kepler, C. E., and Sanlorenzo, E.: A Study of Shock Wave Turbulent Boundary Layer Interaction at M = 3. Rep. No. 222 (Contract No. N6-onr-270, Task Order No. 6, Project Number NR-061-049), Dept. Aero. Eng., Princeton Univ., July 1953.

8. Lange, Roy H.: Present Status of Information Relative to the Prediction of Shock-Induced Boundary-Layer Separation. NACA TN 3065, 1954.

9. Gadd, G. E., Holder, D. W., and Regan, J. D.: An Experimental Investigation of the Interaction Between Shock Waves and Boundary Layers. Proc. Roy. Soc. (London), ser. A, vol. 226, no. 1165, Nov. 9, 1954, pp. 227-253.

10. Crocco, Luigi, and Probstein, Ronald F.: The Peak Pressure Rise Across an Oblique Shock Emerging From a Turbulent Boundary Layer Over a Plane Surface. Rep. 254 (Contract N60onr-270, Task 6), Princeton Univ., Dept. of Aero. Eng., Mar. 1954.
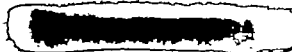
11. Stalder, Jackson R., and Nielsen, Helmer V.: Heat Transfer From a
    Hemisphere-Cylinder Equipped With Flow-Separation Spikes. NACA
    TN 3287, 1954.

12. Chauvin, Leo T.: Aerodynamic Heating of Aircraft Components.
    NACA RM L55L19b, 1956. .

13. McLellan, Charles H., Williams, Thomas W., and Beckwith, Ivan E.:
    Investigation of the Flow Through a Single-Stage Two-Dimensional
    Nozzle in the Langley 11-Inch Hypersonic Tunnel. NACA TN 2223,
    1950.

14. Stine, Howard A., and Wanlass, Kent: Theoretical and Experimental
    Investigation of Aerodynamic-Heating and Isothermal Heat-Transfer
    Parameters on a Hemispherical Nose With Laminar Boundary Layer at
    Supersonic Mach Numbers. NACA TN 3344, 1954.

15. Crawford, Davis H., and McCauley, William D.: Investigation of the
    Laminar Aerodynamic Heat-Transfer Characteristics of a Hemisphere-
    Cylinder in the Langley 11-Inch Hypersonic Tunnel at a Mach Number
    of 6.8. NACA TN 3706, 1956.

16. Bertram, Mitchel H.: Exploratory Investigation of Boundary-Layer
    Transition on a Hollow Cylinder at a Mach Number of 6.9. NACA
    TN 3546, 1956.

17. Van Driest, E. R.: Investigation of Laminar Boundary Layer in
    Compressible Fluids Using the Crocco Method. NACA TN 2597, 1952.

18. Van Driest, E. R.: The Turbulent Boundary Layer With Variable
    Prandtl Number. Rep. No. AL-1914, North American Aviation, Inc.,
    Apr. 2, 1954.

NACA RM L56F22
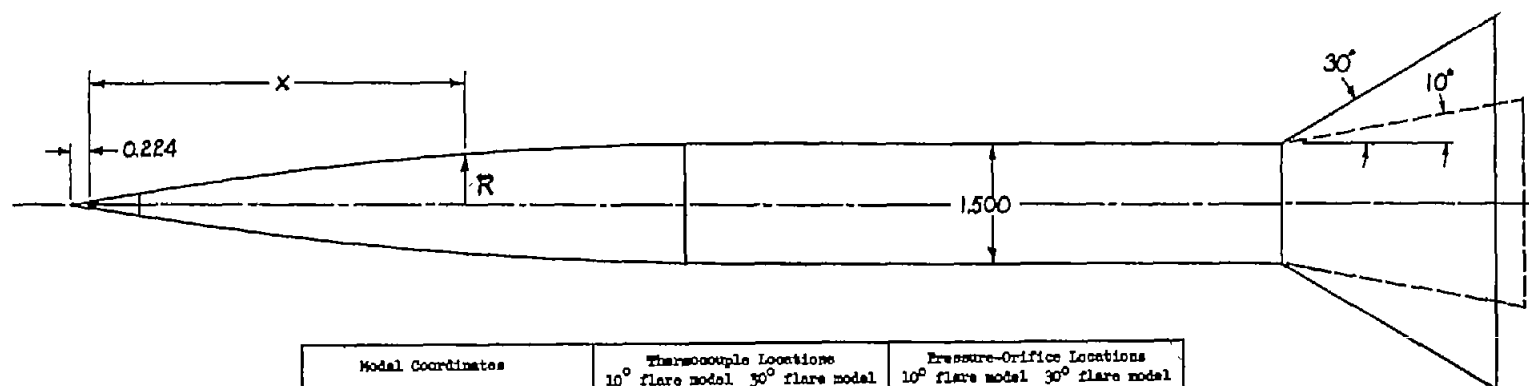
Model Coordinates		Thermocouple Locations		Pressure-Orifice Locations	
		10° flare model	30° flare model	10° flare model	30° flare model
x	R	x	x	x	x
-0.224	0	1.13	1.13	0.75	0.75
0	---	2.13	2.13	2.25	2.25
.625	0.190	3.13	3.13	4.13	4.13
.75	.171	4.13	4.13	4.00	4.00
1.00	.211	5.13	5.13	7.13	7.13
1.50	.283	6.13	6.13	7.78	7.78
2.00	.347	7.13	7.13	---	9.63
2.50	.405	7.50	7.50	10.40	10.45
3.00	.459	7.88	7.88	---	11.34
3.50	.508	8.25	8.25	---	12.50
4.00	.553	8.75	8.63	13.40	13.40
4.50	.594	9.50	9.50	14.51	14.51
5.00	.631	10.37	10.37	15.27	15.34
5.50	.665	11.25	11.25		15.68
6.00	.695	---	11.68	16.02	16.02
6.50	.720	12.00	12.00	---	16.40
7.00	.739	---	12.38	16.77	16.72
7.50	.750	12.75	12.75		
10.00	.750	13.25	13.50		
15.00	.750	13.75	13.88		
18.089	1.295 (10° flare)	14.25	14.25		
17.716	2.317 (30° flare)	14.63	14.63		
		15.00	15.00		
		15.38	15.33		
		15.75	15.67		
		16.12	16.00		
		16.50	16.33		
		16.88	16.67	All dimensions in inches.	
		17.25	17.00		
		17.63	17.33		

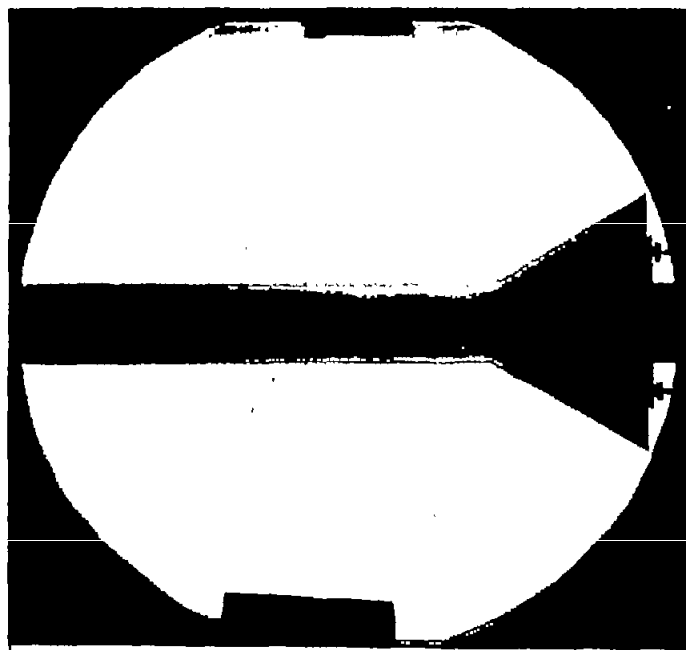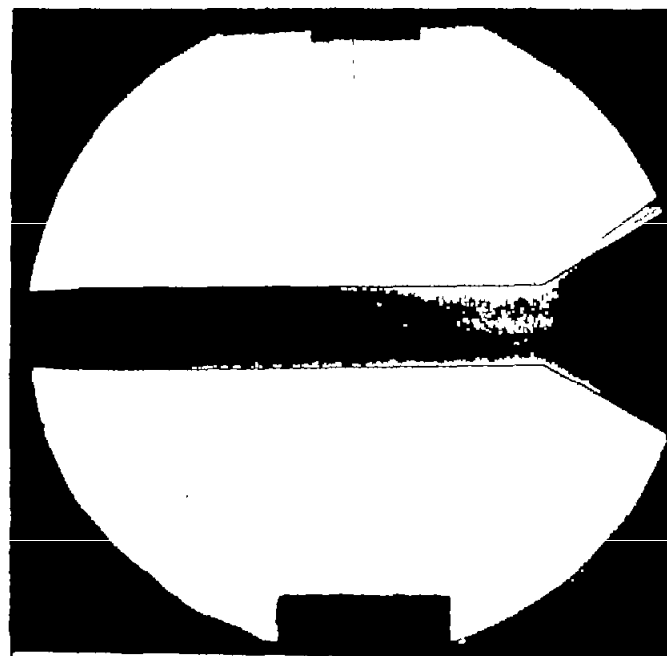Figure 1.- Model dimensions and thermocouple and pressure-orifice locations.
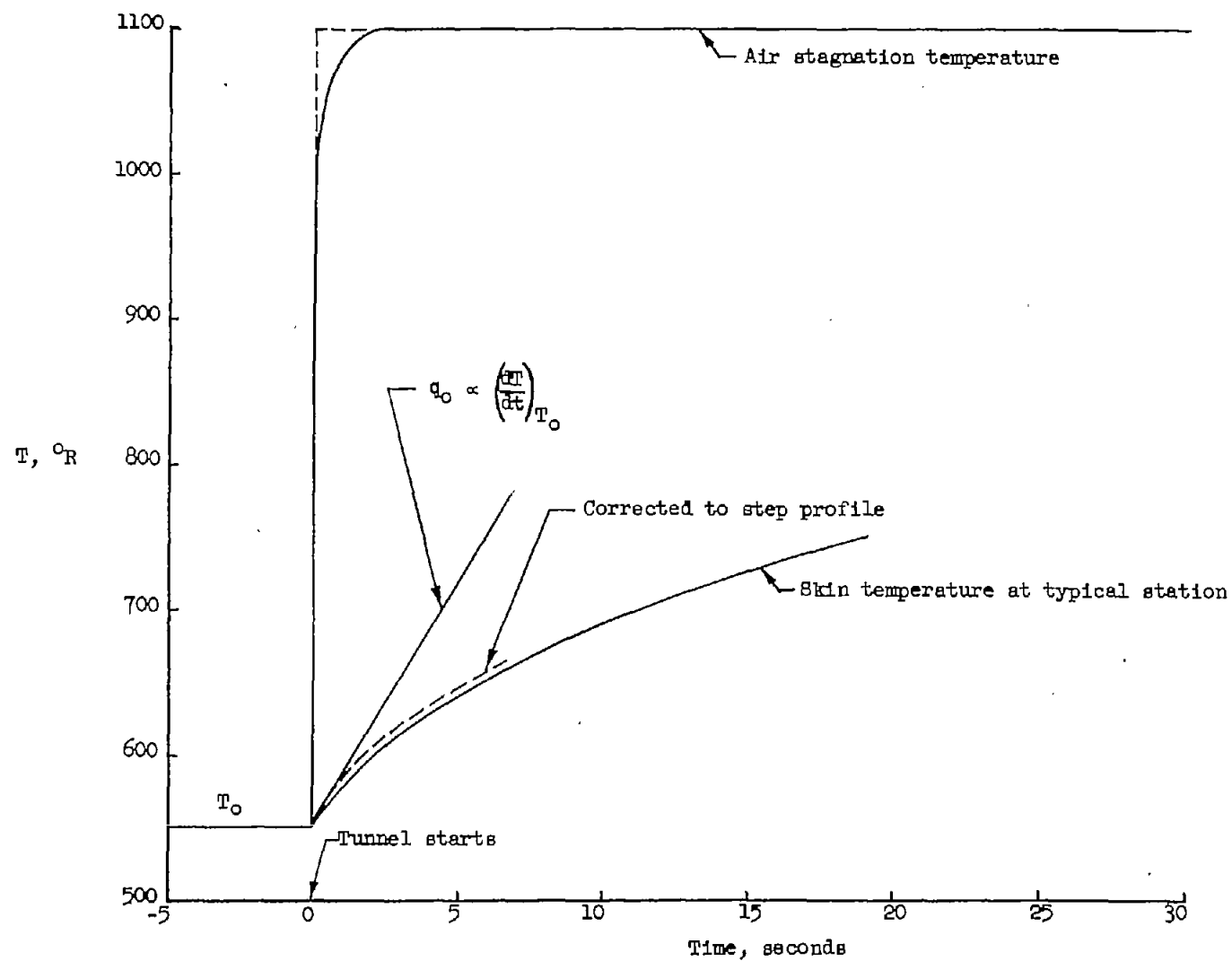
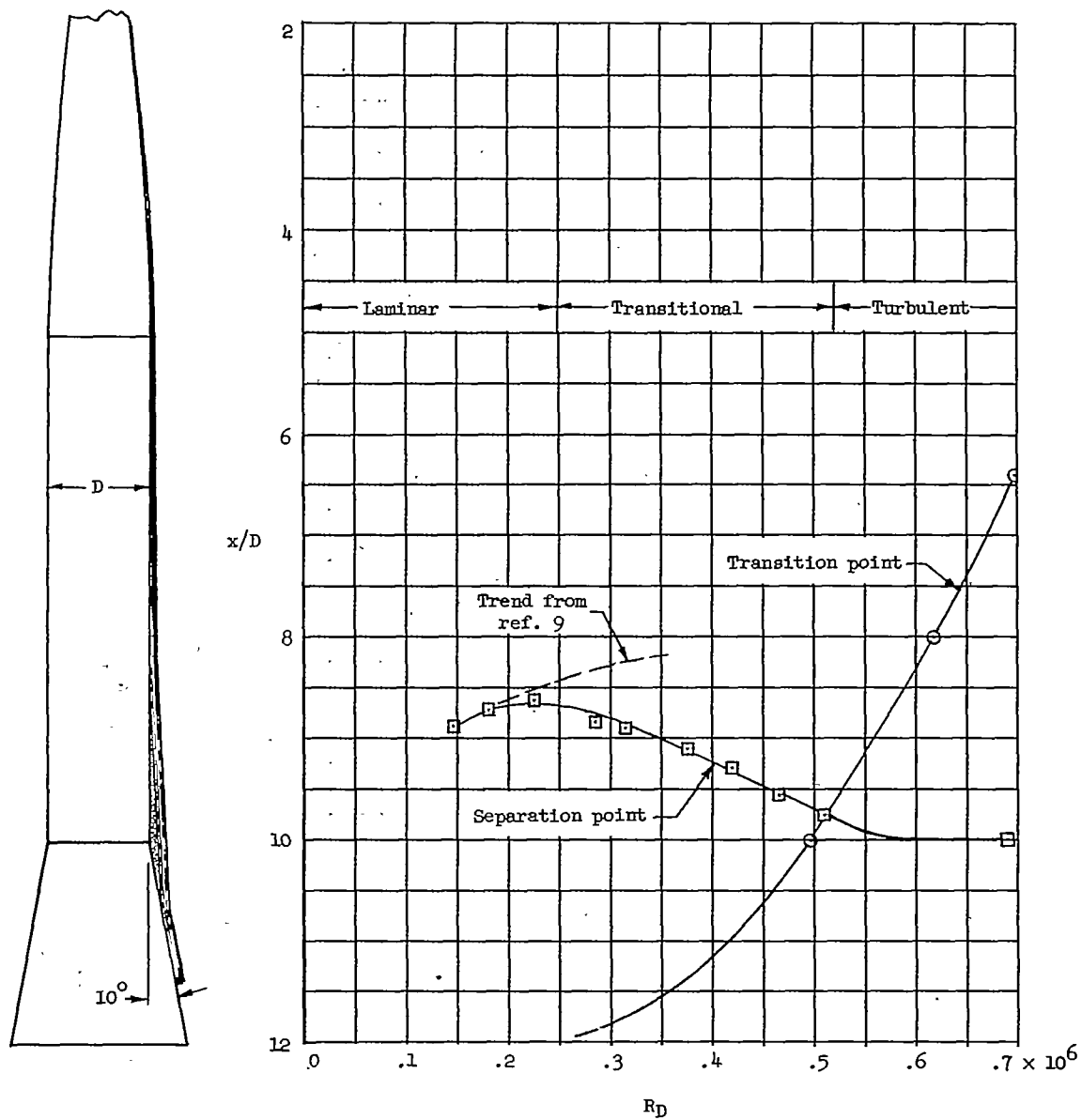Figure 2.- Method of heat-transfer measurement.

$$R_L = 1.8 \times 10^6$$

$$R_L = 8.3 \times 10^6$$

Figure 3.- Schlieren photographs of separated and unseparated flow.   L-93543

(a) 10° flare.

Figure 4.- Effect of Reynolds number on mean positions of the separation
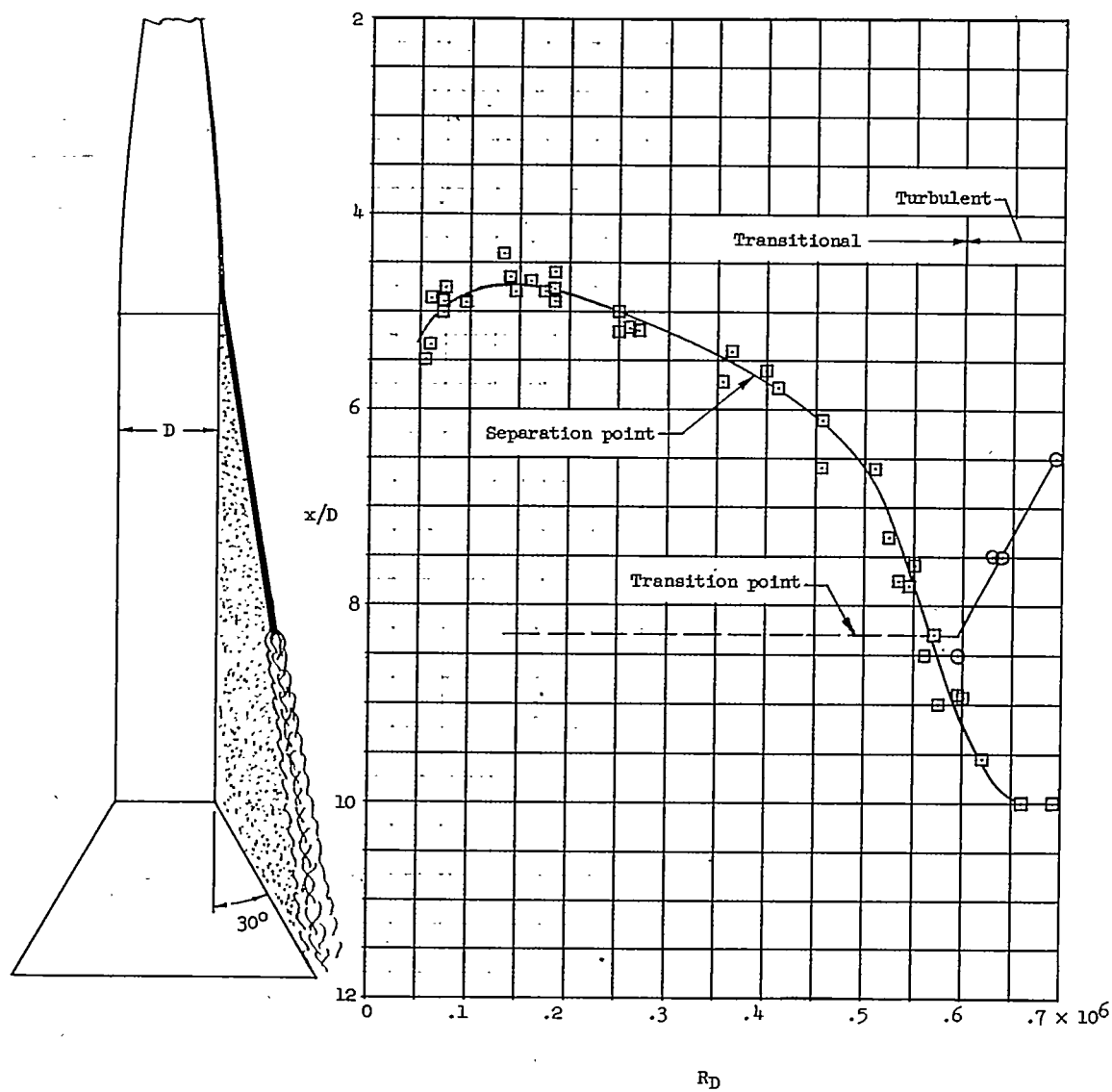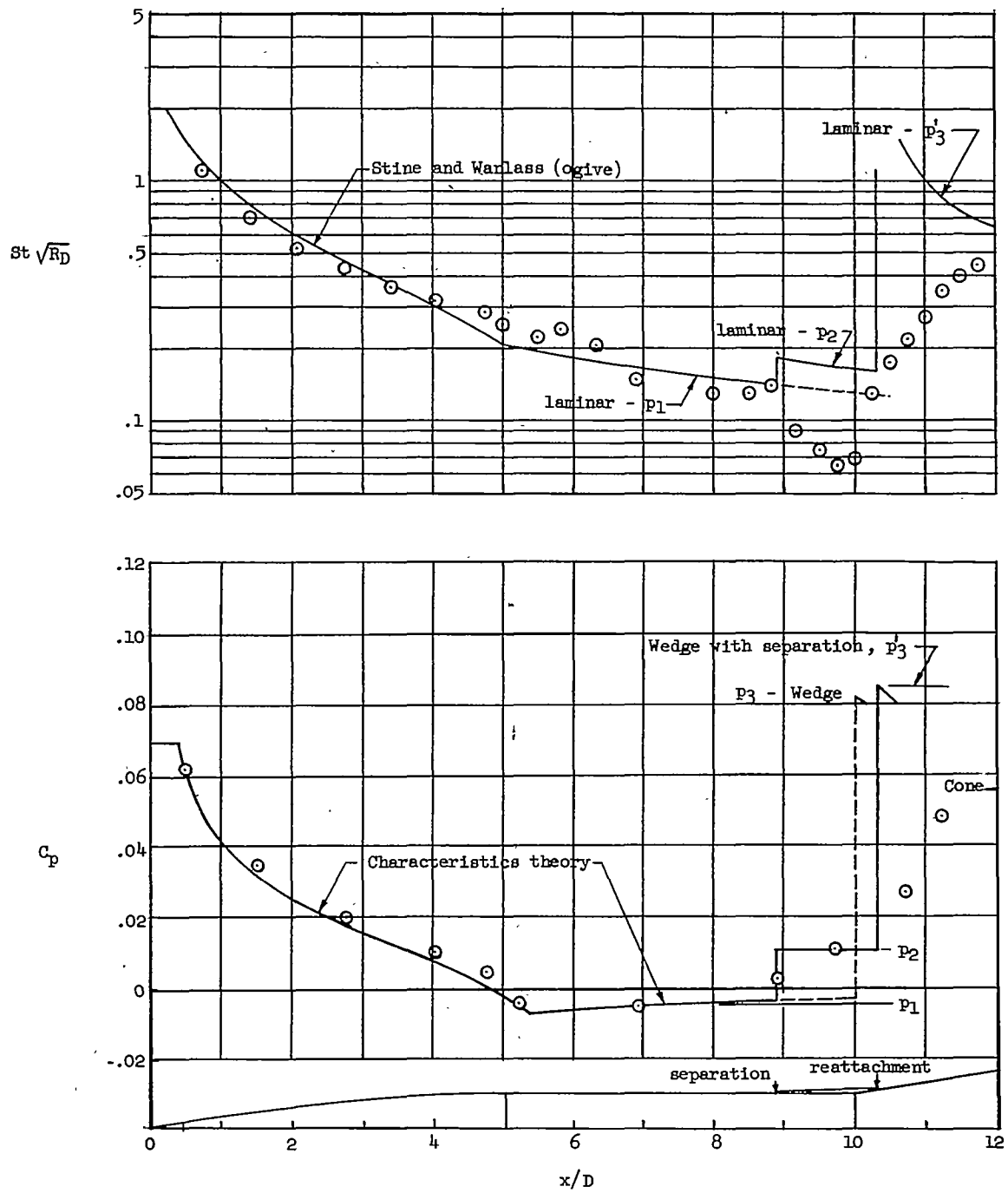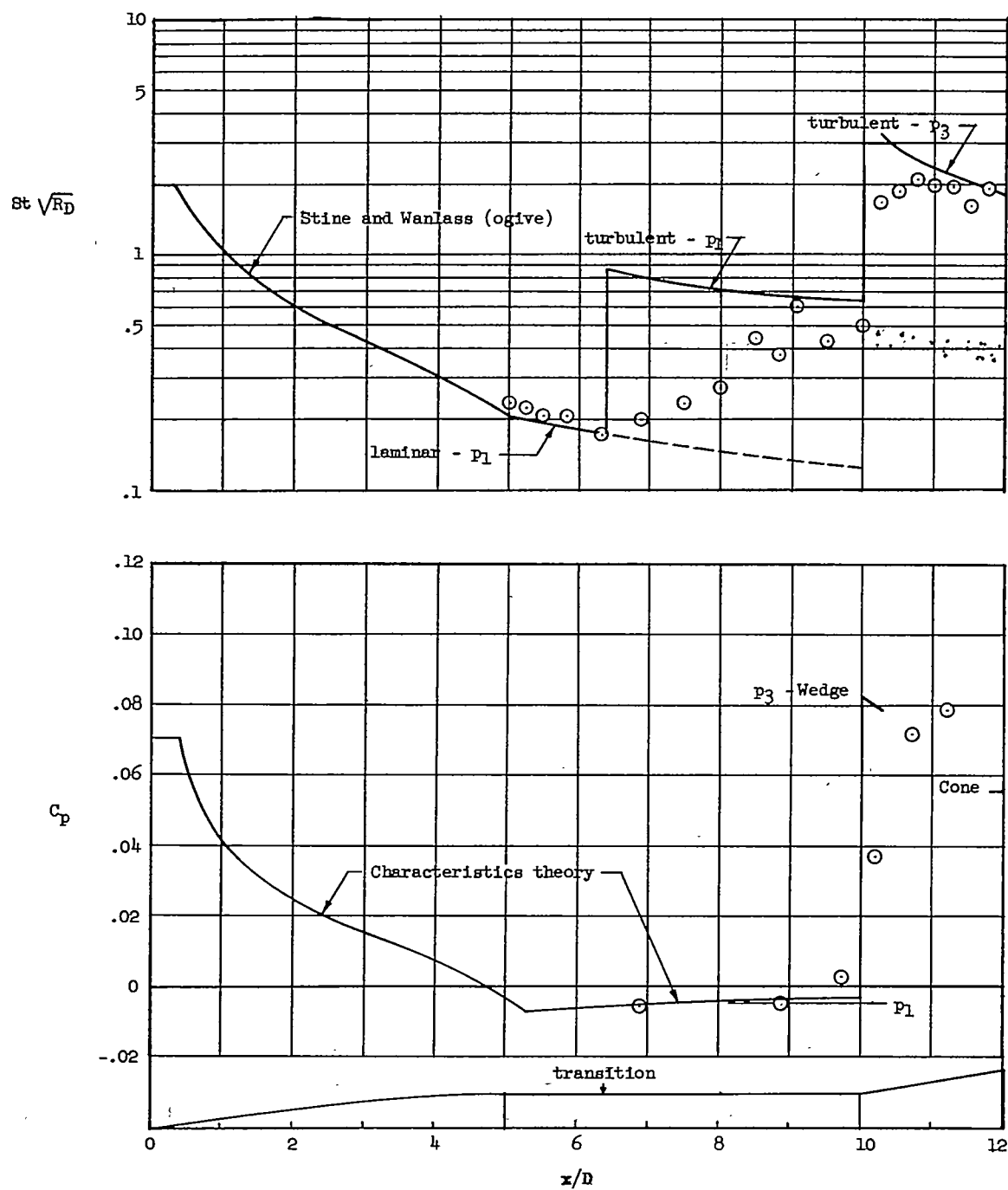point and the start of transition.

NACA RM L56F22

(b) 30° flare.

Figure 4.- Concluded.
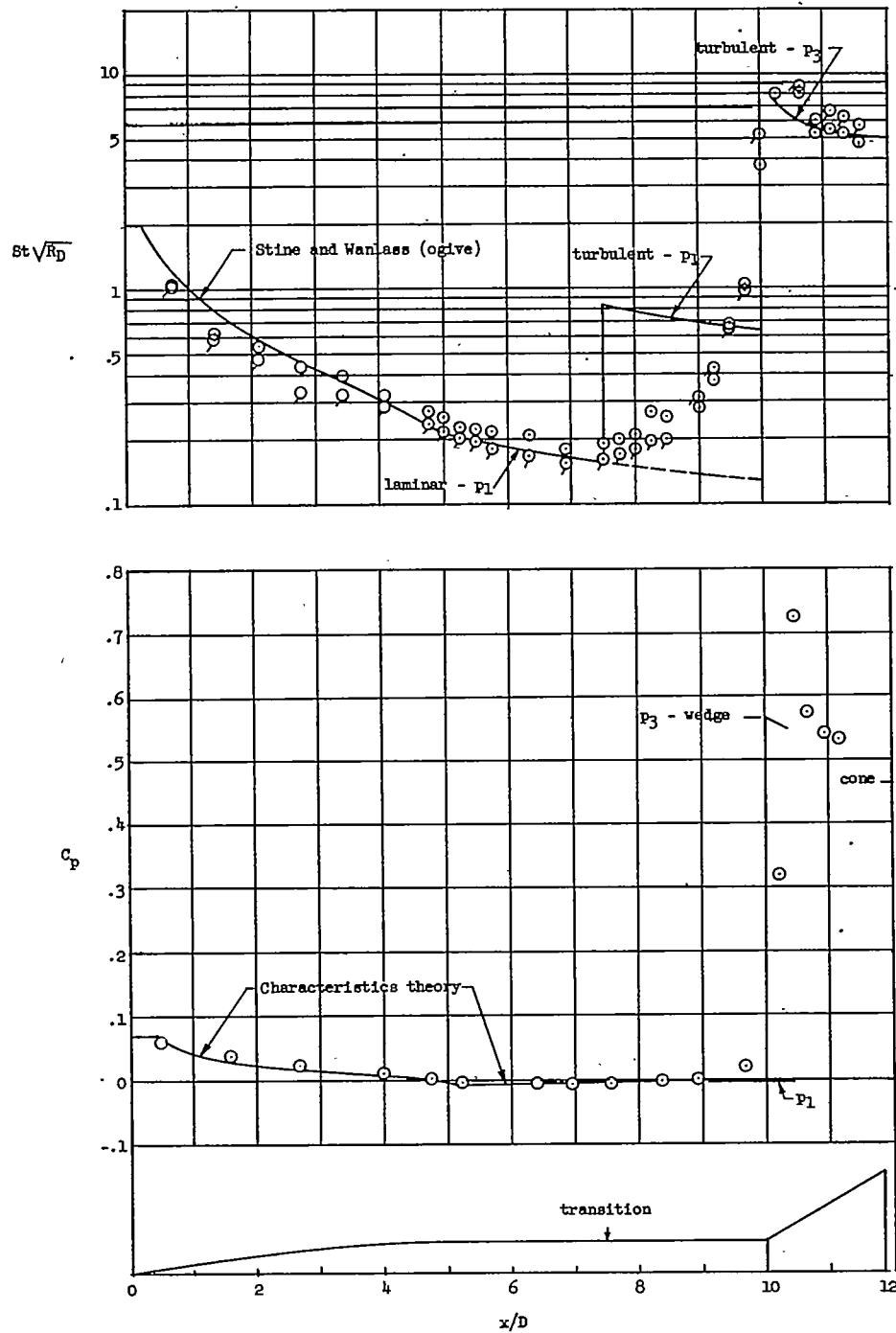
(a) 10° flare, $R_D \approx 0.19 \times 10^6$.

Figure 5.- Heat transfer and pressure distribution.

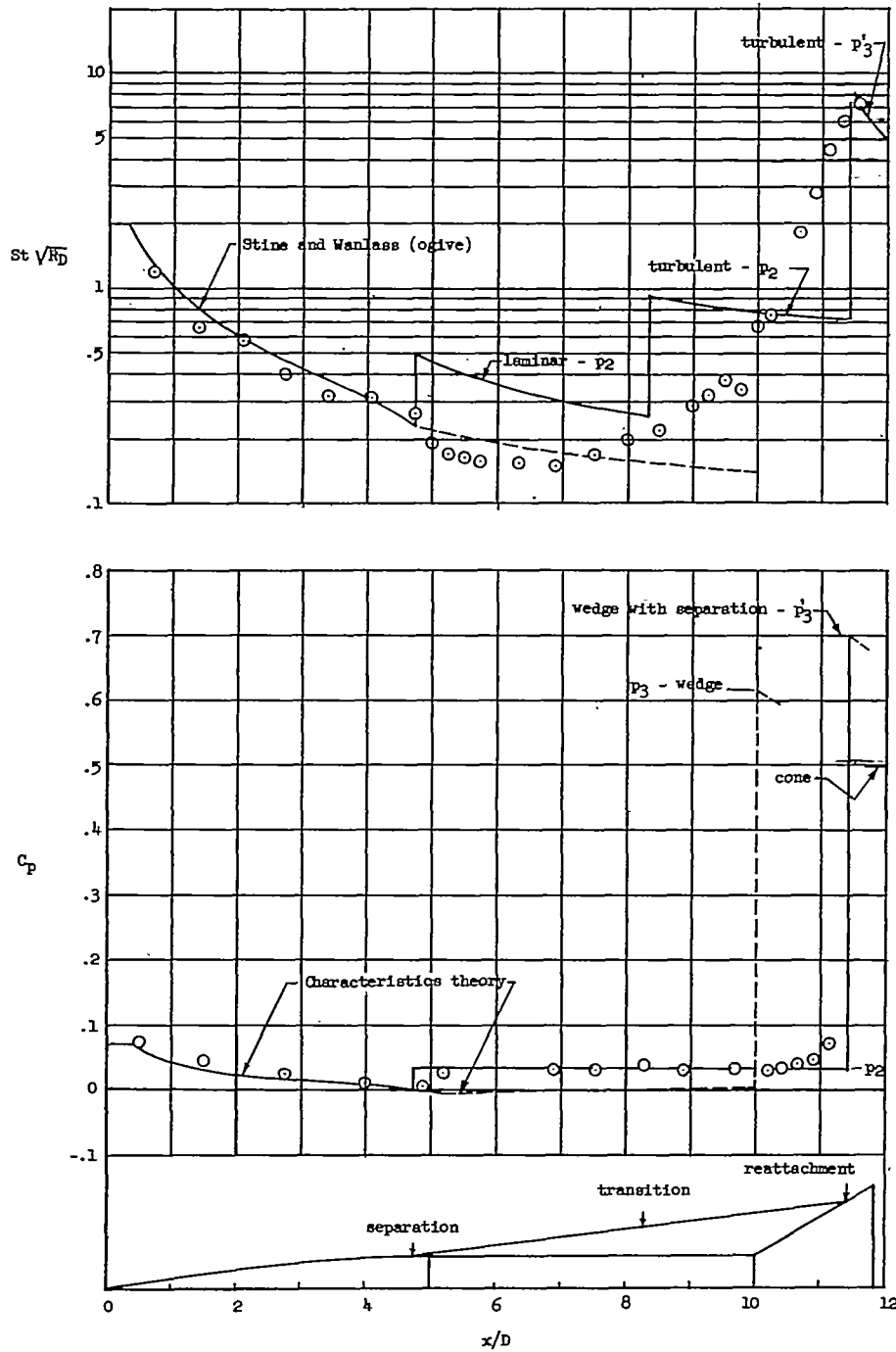(b) $10°$ flare, $R_D \approx 0.70 \times 10^6$.

Figure 5.- Continued.

(c)   30° flare, $R_D \approx 0.63 \times 10^6$.

Figure 5.- Continued.

CONFIDENTIAL

(d) $30°$ flare, $R_D \approx 0.14 \times 10^6$.

Figure 5.- Concluded.

CONFIDENTIAL

Experimental Data
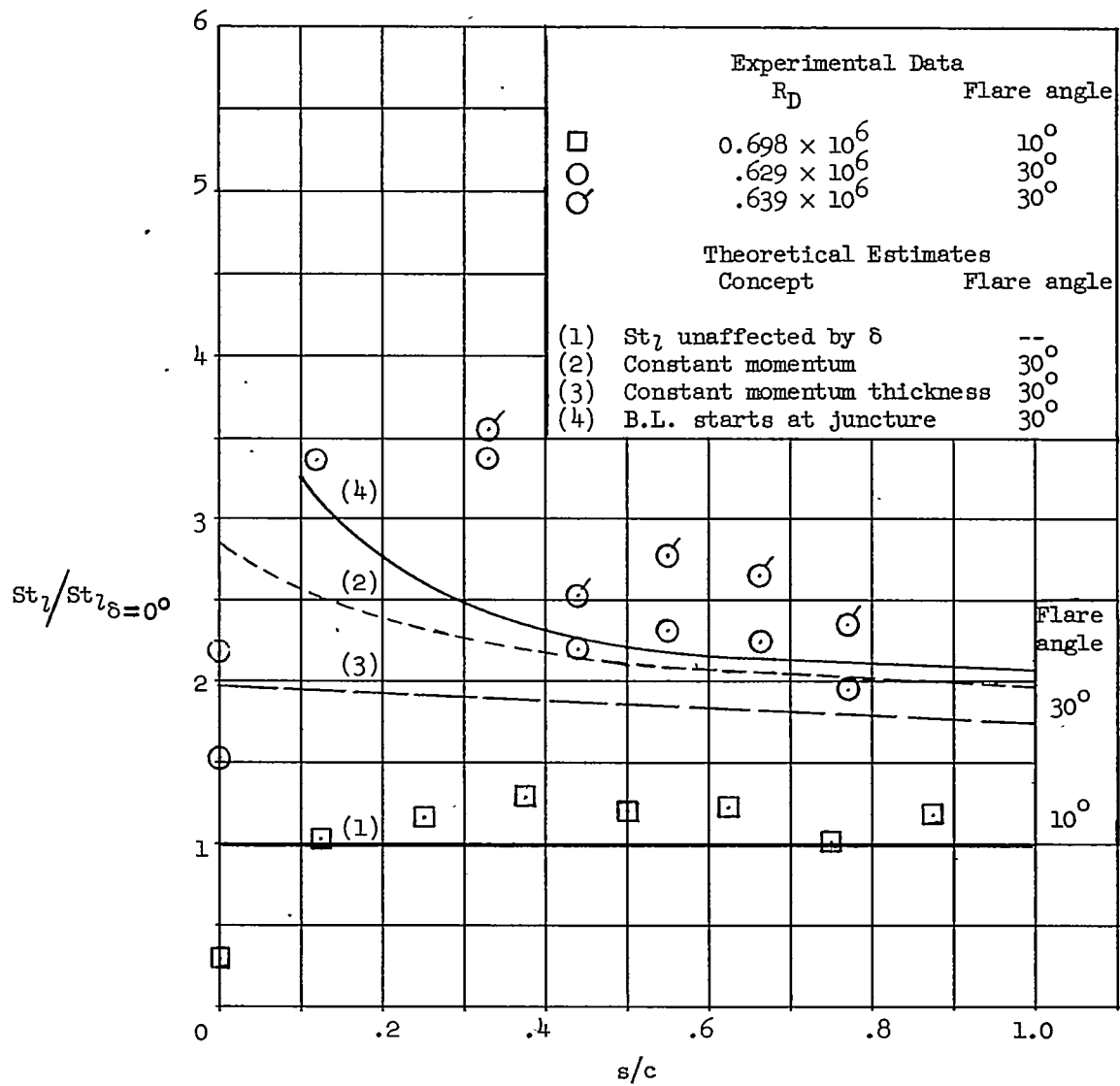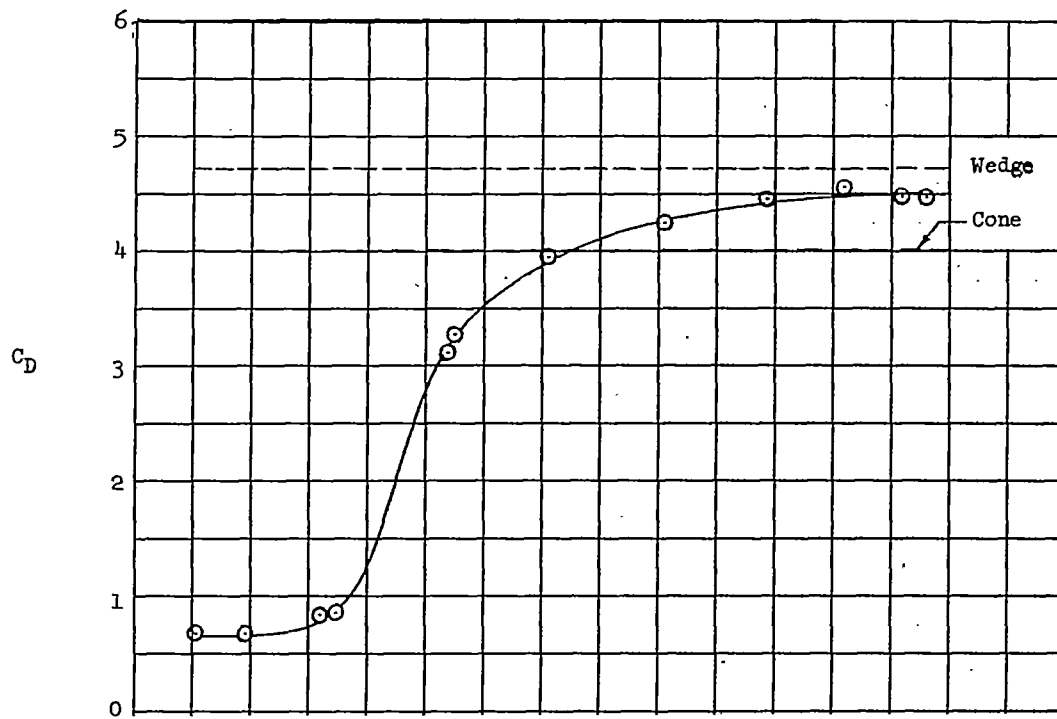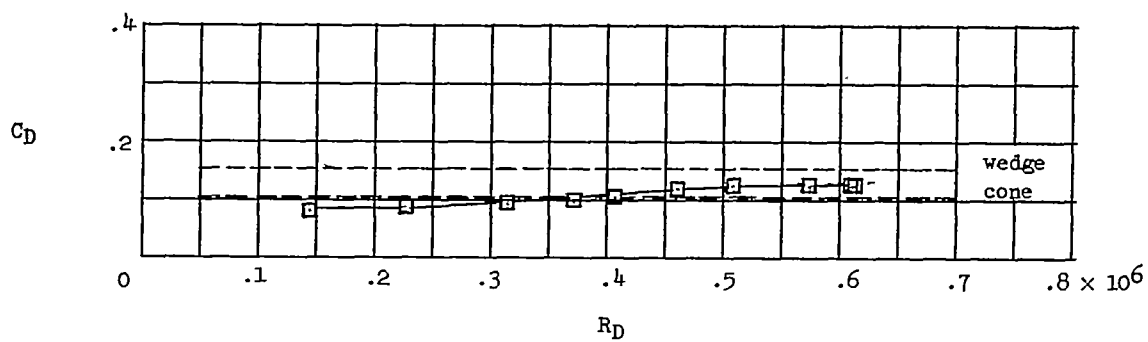
	R_D	Flare angle
□	0.698×10^6	$10°$
○	$.629 \times 10^6$	$30°$
○	$.639 \times 10^6$	$30°$

Theoretical Estimates

	Concept	Flare angle
(1)	St_l unaffected by δ	--
(2)	Constant momentum	$30°$
(3)	Constant momentum thickness	$30°$
(4)	B.L. starts at juncture	$30°$

$St_l \big/ St_{l_{\delta=0°}}$

(4)

(2)

(3)

(1)

Flare angle

$30°$

$10°$

0   .2   .4   .6   .8   1.0

s/c

Figure 6.- Local heat-transfer coefficients on flare.

(a) 30° flare.

(b) 10° flare.

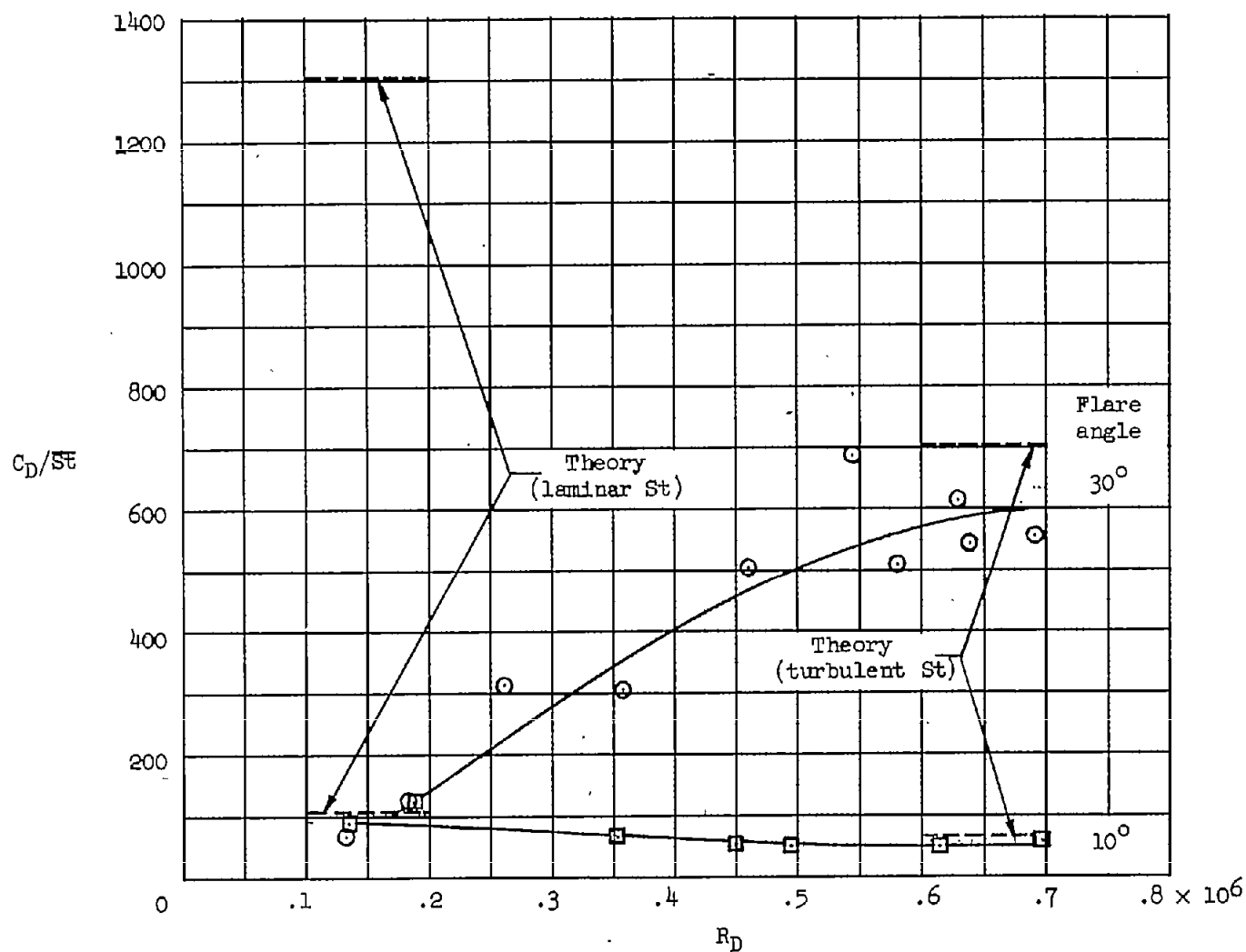Figure 7.- Variation of flare pressure drag with Reynolds number.

Figure 8.- Variation of the ratio of flare pressure drag to flare mean heat-transfer coefficient with Reynolds number.